Ammonia Synthesis from Electrochemical Reduction of Nitrate Using Boron-Doped Diamond Electrodes

Ammonia Synthesis from Electrochemical Reduction of Nitrate by Using Boron-doped Diamond Electrodes

Satoru Kuramochi, Andrea Fiorani,* Yasuaki Einaga*

Department of Chemistry, Keio University, 3-14-1 Hiyoshi, Yokohama 223-8522, Japan

KEYWORDS: ammonia; boron-doped diamond; nitrate; reduction; kinetics constant

ABSTRACT: In this study, we investigated the ammonia synthesis from electrochemical nitrate reduction by using a boron-doped diamond (BDD) electrode. Several parameters were optimized, including the boron doping level in BDD, reduction potential, cell type, and electrolyte, to reach an ammonia production rate of 67±12 μmol cm^{-2} h^{-1} with a faradaic efficiency of 98±6%. The ammonia production rate could be enhanced up to 184 μmol cm^{-2} h^{-1} by adjusting the boron doping level. From kinetic measurements during ammonia synthesis, the time dependence of NO_3^-, NO_2^-, and NH_3 concentrations confirmed that the reaction of electrochemical nitrate reduction can be described by two sequential reactions: NO_3^- reduction to NO_2^- and following reduction of NO_2^- to NH_3. Among the conditions studied, the addition of NaOH, that decreased the charge transfer resistance of electron transfer and increased the ionic conductivity, was found to enhance the rate constant of both reactions, with a significantly larger effect on NO_2^- to NH_3. In addition, comparison with other electrode materials, namely Cu, Ti, and glassy carbon confirmed the superior quality of BDD electrode in terms of production rate, faradaic efficiency, and durability.

INTRODUCTION

Ammonia (NH_3) is currently one of the most important chemical compounds playing a pivotal and major role as raw material for fertilizers (e.g., urea in the Bazarov synthesis,[1] ammonium phosphate, and ammonium nitrate). In addition, NH_3 finds application in the chemical industry for the synthesis of nitric acid (Ostwald process),[2] hydrazine, cyanides, pharmaceuticals, plastics, textiles, and explosives. Actually, every nitrogen atom in industrially produced chemicals compounds comes directly or indirectly from ammonia.[3] Hypothetical use of NH_3 as fuel (storage and carrier of H_2) has also been suggested.[4] To sustain its demand, mass production of NH_3 is based on the Haber-Bosch process since its inception in 1909.[5,6]

The high-energy demand of the Haber-Bosh process prompted an increasing interest for lower energy intensive methods for ammonia synthesis, and electrochemistry emerged among others, owing ambient temperature and pressure as reaction conditions.

The direct reduction of N_2 gas to NH_3 in aqueous electrolyte has been widely investigated. However, the high stability of the N_2 triple bond (946 kJ mol^{-1}),[7] and the competing hydrogen evolution reaction lead to low or modest faradaic efficiencies, and very poor NH_3 production rates which prevent any possible application.[8] Nitriding,[9] the reaction of lithium, magnesium, alkaline-earth metals, or transition metals of Groups IV-VII with N_2 to form nitrides, has been suggested as possible strategy to overcome these problems. In fact, reaction of N_2 over a Li salt reduced to Li metal at the electrode produces LiN_3 which following hydrolysis affords NH_3. The production rates by this strategy are promising,[10] but the already high pressure on lithium resources by the Li-ion battery sector[11] will hardly make this method to reach any practical development.

Electrochemical synthesis of NH_3 can occur also during nitrate reduction that it is known since 1902 from works of Julius Tafel,[12] and more prominently in the 1990s from researches on nitrate removal in groundwater for environmental remediation. In such cases, the optimal result is N_2 gas production that finally leaves the solution.[13,14] Beside polluted groundwater contaminated by nitrate,[15] mainly from fertilizer due to insufficient nitrification/denitrification,[16] different source of nitrate are found in nuclear,[17,18] industrial,[19] and textile[20] wastewaters.

The advantage of this strategy is twofold, while producing NH_3, at the same time the wastewater can be decontaminated from nitrate.

However, a concomitant challenge lies in the multiplicity of partially reduced species which can be generated through this reaction, before reaching the fully reduced NH_3 (i.e., NO_2^-, NO_2, NO, N_2O, N_2, NH_2OH, NH_2NH_2, NH_3). Although nitrite, nitrogen gas, and ammonia can be regarded as main products (eqs 1–4).[21]

$$NO_3^- + 3H^+ + 2e^- \rightarrow HNO_2 + H_2O \qquad E^0 = 0.934\ V \quad (1)^{22}$$

$$2NO_3^- + 12H^+ + 10e^- \rightarrow N_2 + 6H_2O \qquad E^0 = 1.246\ V \quad (2)^{22}$$

$$NO_3^- + 10H^+ + 8e^- \rightarrow NH_4^+ + 3H_2O \qquad E^0 = 0.880\ V \quad (3)^{23}$$

$$HNO_2 + 7H^+ + 6e^- \rightarrow NH_4^+ + 2H_2O \qquad E^0 = 0.864\ V \quad (4)^{22}$$

Generally, in electrochemical synthesis, the selectivity toward the product of interest can be tuned by careful selection of solvents, supporting electrolytes, and in particular the electrode materials or electrocatalysts. Many kinds of materials have been investigated, such as polycrystalline Cu and copper oxide,[24-26] or in combination with other metals such as Co,[27,28] Zn,[29] Ni,[30]

or Rh,[31] and also Ga/In/Sn eutectic,[32] Fe,[33,34] Rh,[35] Ni-Rh,[36] Ag,[37] Co,[38] Pd/TiO_2[39] and Co_3O_4/TiO_2.[40]

However, metal electrodes and especially electrocatalysts with hierarchical and complex structures are prone to loss of activity by corrosion that induces structural changes or metal dissolution with consequent impact on efficiency, production rate, durability/cost, and safety concerns about metal leaching.[41]

Here, we propose a sp^3 carbon-based electrode, namely boron-doped diamond (BDD)[42-45] that possesses high physical and chemical stability, and wide potential window that results from low activity toward protons reduction, a competing reaction during nitrate reduction.

These characteristics made BDD electrode useful for other electrochemical reduction reactions, for example CO_2 to formic acid or CO.[46-50]

Moreover, the doping element boron does not pose safety risk, in principle, being also a necessary element for human health,[51] contrary to heavy metals of some electrocatalysts.

In the following investigation, we explore the conditions for efficient ammonia synthesis from nitrate reduction at BDD electrode by optimizing the boron doping concentration in the BDD, reduction potential, electrochemical cell configuration, and electrolyte composition. Kinetic and electrochemical impedance spectroscopy measurements were performed to get insight into the electrochemical reduction mechanism of nitrate to ammonia.

EXPERIMENTAL SECTION

Chemicals and materials. $NaNO_3$, NaOH (Wako, Japan). Acetone and trimethoxyborane (TCI, Japan). Glassy carbon, copper, titanium and platinum electrodes (Nilaco Co, Japan). Nafion membrane NRE-212 (Sigma-Aldrich). Deionized water with resistivity of 18.2 MΩ·cm at 25°C (DIRECT-Q3 UV Water Purification System, Millipore). All reagents were commercially available and used without further purification. Details are available in paragraph 1 in the Supporting Information.

Fabrication of boron-doped diamond. BDD was deposited on silicon (100) wafers by using a microwave plasma-assisted chemical vapor deposition (MPCVD), from a solution of acetone and trimethyl borate, with a B/C atomic ratio of 0.1, 0.2, 0.5, and 1%. The BDD morphology and quality were confirmed by SEM and Raman spectroscopy measurements (Figure S1 and S2). Details are available in paragraph 2 in the Supporting Information.

Electrochemistry. Undivided batch cell, divided batch cell and divided flow cell were compared (Figure S3). In divided cells, anode chamber and cathode chamber were separated by a 0.002 inch Nafion membrane. Working electrode (WE) was a BDD, counter electrode was a Pt plate, and reference electrode was Ag/AgCl (KCl saturated) which all potentials are referred throughout the manuscript, unless otherwise stated. Details are available in paragraph 3 in the Supporting Information.

Products quantification. Absorption spectrophotometry methods were used for the determination of NO_3^-, NO_2^- and NH_3. Production rate (μmol cm^{-2} h^{-1}) and faradaic efficiency (FE) were used as figure of merit to assess the results of nitrate reduction to ammonia.

Details are available in paragraphs 4 and 5 in the Supporting Information (Figure S4–S6).

RESULTS AND DISCUSSION

Boron doping concentration

Diamond is a semiconductor (indirect band gap 5.4 eV)[52] which optical, physical, and electrochemical properties are highly affected by heteroatom doping, generally boron.[42] In particular, around 2-3×10^{20} [B]cm^{-3} is found the threshold for metal conductivity[53] which is therefore the interesting region to explore for electrochemical applications. We prepared four BDD electrodes at different boron doping concentrations, namely 0.1, 0.2, 0.5, and 1% of B/C ratio to evaluate the effect of boron doping on nitrate reduction current, and proton reduction current (i.e., the competing hydrogen evolution reaction). The best boron doping concentration would maximize nitrate reduction and minimize protons reduction. Experimentally, linear sweep voltammetry has been compared in 0.1 M NaCl and 0.1 M $NaNO_3$ at the same pH which should resemble only hydrogen reduction, and hydrogen reduction plus nitrate reduction, respectively (Figure 1).

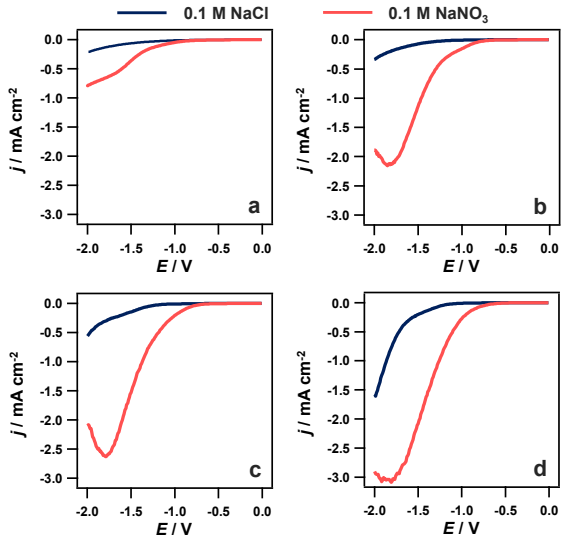

Figure 1. Liner sweep voltammograms at 10 mV s^{-1} in aqueous 0.1 M NaCl (pH 5.9, blue line) or 0.1 M $NaNO_3$ (pH 5.8, red line) by using BDD electrodes with boron concentration of 0.1% (a), 0.2% (b), 0.5% (c), and 1% (d). Undivided batch cell, stirring rate 2912 rpm. WE: 12.56 cm^2. V *vs* Ag/AgCl (KCl sat.).

The larger current for nitrate reduction compared to the hydrogen reduction confirms the low catalytic activity of BDD toward protons reduction and its beneficial role for electrochemical reduction reactions in aqueous electrolytes. The level of boron doping affects the surface conductivity of the BDD and consequently the rate of electron transfer.[54] In fact, the current, both in NaCl and $NaNO_3$, increase accordingly. However, the current for hydrogen evolution increases linearly with the boron doping concentration, while the process begin to be limited by nitrate concentration between B/C 0.5 and 1%. On the contrary, 0.1% BDD in $NaNO_3$ had no peak, but it reached an almost stationary state because at this boron concentration the electron transfer was slower that the diffusion process of nitrate.

This resulted in 91% of the current for nitrate reduction on 0.2% BDD (at –1.8 V), the highest percentage among the four BDD electrodes that is consequently selected for the following experiments (Table S1).

Optimal reduction potential

Electrochemical nitrate reduction was performed at different potentials to confirm the best faradaic efficiency and production rate of NH_3 (Figure 2).

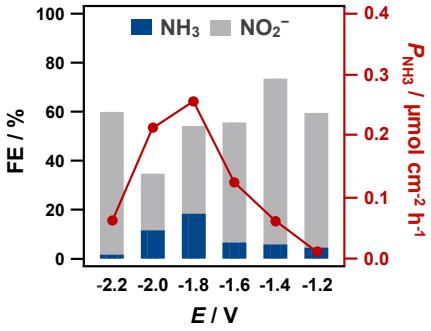

Figure 2. Potential dependence of FE for NH_3 (blue) and NO_2^- (gray). Potentiostatic reduction of 0.1 M $NaNO_3$ by using 0.2% BDD electrode for 1 h. Divided flow cell, flow rate 200 mL min^{-1}. WE: 9.616 cm^2. V *vs* Ag/AgCl (KCl sat.).

The maximum faradaic efficiency of NH_3 (FE_{NH3}) reached 18.3% at –1.8 V, with a NH_3 production rate (P_{NH3}) of 0.258 μmol cm^{-2} h^{-1} that follows the same trend of FE_{NH3} (Figure S7). Increasing the reduction potential from –1.2 V to –1.8 V enabled a more efficient ammonia production as the FE_{NH3} and P_{NH3} became larger. This is paired with a lower FE for nitrite implying that this intermediate is reduced to NH_3 by a following reaction.

Excessively negative potential beyond –1.8 V resulted in a decrease in both FE_{NH3} and P_{NH3} as result of higher hydrogen evolution, and reduction to N_2.[55] At –2.2 V, the FE_{NO2-} increased significantly, also the current density (Figure S8). Because the formation of NH_3 requires protons, and these are mainly reduced to hydrogen, the reduction of nitrate will likely to stop at the nitrite intermediate. Based on these results, electrolysis was performed using a potential of –1.8 V for the following experiments.

Electrochemical cell configuration

Before moving to mechanism investigation and process optimization, three types of electrochemical cell were compared, to achieve a stable electrochemical system by controlling the mass transfer regime. These comprised (i) an undivided batch cell, (ii) a divided batch cell, and (iii) a divided flow cell. Both batch cells were equipped with a PTFE rod connected to an electrical motor to control the stirring conditions (Figure S3).

The divided batch cell reached the highest FE_{NH3} and P_{NH3} of 46.1% and 8.33 μmol cm^{-2} h^{-1}, respectively (Figure S9 and S10). The low FE of undivided batch cell (7.99%) can be the result of NH_3 oxidation at the counter electrode. The FE_{NH3} in divided flow cell was 18.3%, about half that of divided batch cell. The nitrate reduction reaction is a mass transfer limited reaction, in fact, even with high rotation speed is possible to observe a transient current signal in the linear sweep voltammetry that does not attain a stationary state (Figure S11). For these reasons, electrochemical nitrate reduction was performed under intense stirring that enables a high FE_{NH3} by supplying nitrate and decreasing the competing proton reduction, furthermore increasing the P_{NH3} (Figure S12 and S13).

Electrolyte engineering

In principle, the condition of controlled pH by addition of salts to buffer the solution cannot be easily implementable in view of application, but it is fundamental to understand the mechanism and optimal reaction conditions. To investigate the pH of electrolyte that is suitable for NH_3 synthesis, the electrochemical nitrate reduction was conducted in phosphate buffer (Figure 3).

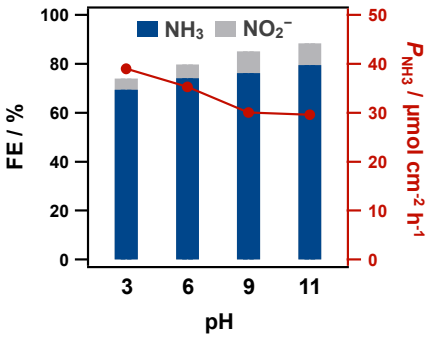

Figure 3. pH dependence of FE for NH_3 (blue) and NO_2^- (gray), and P_{NH3} (red). Potentiostatic reduction at –1.8 V vs Ag/AgCl (KCl sat.) of 0.1 M $NaNO_3$ added with 0.2 M phosphate by using 0.2% BDD electrode for 1 h. Divided batch cell, stirring rate 2912 rpm. WE: 12.56 cm^2.

FE_{NH3} and P_{NH3} had two opposite responses to pH as it increased from 3 to 11: while FE_{NH3} increased from 69.4 to 79.5% (ΔFE=+14.6%), the P_{NH3} decreased from 38.9 μmol cm^{-2} h^{-1} to 29.60 μmol cm^{-2} h^{-1} (ΔP_{NH3}=–23.9%) As the concentration of protons become high, hydrogen evolution is more easy to occur which diverts the current from nitrate reduction lowering the FE. On the other hand, nitrate reduction to ammonia requires protons and their low availability at high pH can be the rate determining factor for the smaller reduction current (Figure S14), and therefore low P_{NH3}.

The value of ΔFE_{NH3} and ΔP_{NH3} are not very different, therefore the pH does not suggest clearly which value should be selected. However, we noticed that addition of the phosphate electrolyte increased the steady state current from 4 mA cm^{-2} (Figure S13) to 12 mA cm^{-2} (Figure S14) at the same pH ~6. Therefore, the suitable approach can be alkaline pH for a high FE and addition of supporting electrolyte to reach higher currents which has been investigated for different concentrations of NaOH up to 1 M (Figure 4).

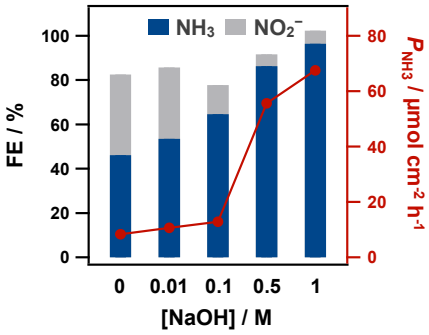

Figure 4. FE for NH_3 (blue) and NO_2^- (gray), and P_{NH3} (red). Potentiostatic reduction at –1.8 V vs Ag/AgCl (KCl sat.) of 0.1 M $NaNO_3$ added with NaOH by using 0.2% BDD electrode for 1 h. Divided batch cell, stirring rate 2912 rpm. WE: 12.56 cm^2.

The addition of NaOH as supporting electrolyte was beneficial for both FE_{NH3} and P_{NH3} confirming this strategy as effective, although counterintuitive because an electrochemical reduction reaction, which involves proton-electron transfer, should be facilitated in acidic pH. This shares some similarity with the oxygen reduction reaction that is more favorable in alkaline electrolyte.[56,57]

This suggests that although proton concentration can limit the reaction rate, faster electron transfer, which includes also the adsorption of NO_3^- on the electrode is responsible for the increasing P_{NH3}, thus the reduction current (Figure S15).

The FE_{NH3} reached 98±6% and the P_{NH3} 67±12 μmol cm^{-2} h^{-1} (Figure S16).

The sharp increase of P_{NH3} between 0.1 M and 0.5 M NaOH is located exactly in concurrence with the sharp increase of the electrolyte conductivity, from 24 to 71 mS cm^{-1}, reaching 112 mS cm^{-1} for 1 M NaOH (Figure S17).

Addition of other Na salts (chloride, perchlorate, and sulfate) at 1 M concentration did not attain similar results confirming the role of high ionic conductivity and pH for efficient NH_3 synthesis (Figure S18 and S19). Additionally, the structure of the electrical double layer can be responsible for different result when the nitrate should reach the surface of the electrode before the electron transfer which can be hindered by other adsorbed anions. In fact, the ionic conductivity cannot account completely for the difference observed among NaCl, $NaClO_4$ and Na_2SO_4. This is evident in the FE_{NH3} with Na_2SO_4 that is higher than NaCl and $NaClO_4$ despite the lower ionic conductivity.

The effect of the anions is not unanimous and is highly dependent on the electrode material which competitive adsorption may produce an inhibiting, or a strong catalytic effect.[58-61] In addition, anions that favorite hydrogen evolution will impact negatively on NO_3^- reduction that seems the case of NaCl and $NaClO_4$.

To get insight on the effect of hydroxide for reducing NO_3^- to NH_3, we measured linear sweep voltammetry with increasing NaOH concentrations that confirmed a faster reduction reaction, with a positive potential shift and current increase (Figure S20). A more quantitative analysis was conducted by electrochemical impedance spectroscopy that can measure the resistance associated with the electron transfer during NO_3^- reduction (Figure 5, S21 and S22).

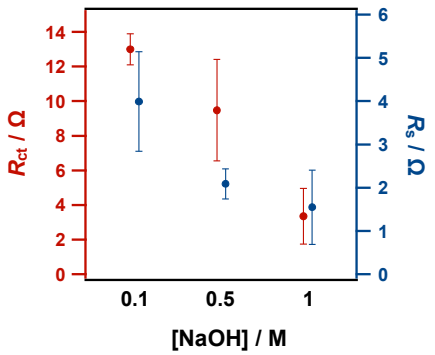

Figure 5. Charge transfer resistance (R_{ct}) and solution resistance (R_s) of 0.1 M $NaNO_3$ added with NaOH at −1.8 V *vs* Ag/AgCl (KCl sat.).

The charge transfer resistance (R_{ct}) decreased with the addition of NaOH that indicates a faster electron transfer for the first reduction of NO_3^- in line with the increasing P_{NH3}. Moreover, the solution resistance (R_s) decreased which resulted in around 100 mV of ohmic drop between 0.1 and 1 M NaOH, although not enough to suggest a variation of the NO_3^- reduction rate based on different potentials.

Interestingly, we noticed that under continuous EIS measurements, the R_{ct} decreases until reaching a stable state implying a modification of the BDD surface (Figure S21).

BDD surface can be terminated by hydrogen under cathodic current[62] which assumes a partial positive charge and could increase the rate of electron transfer facilitating the nitrate adsorption.[63]

This confirm that the NO_3^- reduction is highly affected by the nitrate adsorption on BDD surface and the NaOH has a positive effect on in promoting this process.

Kinetic of electrochemical nitrate reduction

In order to understand the reaction pathway from nitrate to ammonia, the reduction reaction was conducted for 6 hours.

When electrochemical nitrate reduction was performed in 0.1 M $NaNO_3$, the concentration of nitrite increased faster than ammonia.

On the other hand, when the reduction reaction was conducted with the addition of 1 M NaOH, the opposite outcome was observed, as the ammonia concentration increased faster that the nitrite which also reached a steady state.

Starting with 100 mM of nitrate, the sum of nitrate, nitrite, and ammonia concentration fell below 95 mM after 3 hours (without NaOH) and 2 hours (with NaOH) suggesting the formation of different reduced species, most likely hydrogen, or leaking of ammonia when it reached high concentrations because the system is not gas tight (*vide infra*). For this reason, the kinetic analysis was limited at the beginning of the nitrate reduction for total concentration above 95 mM (Figure 6, S23), in the range of product quantification error.

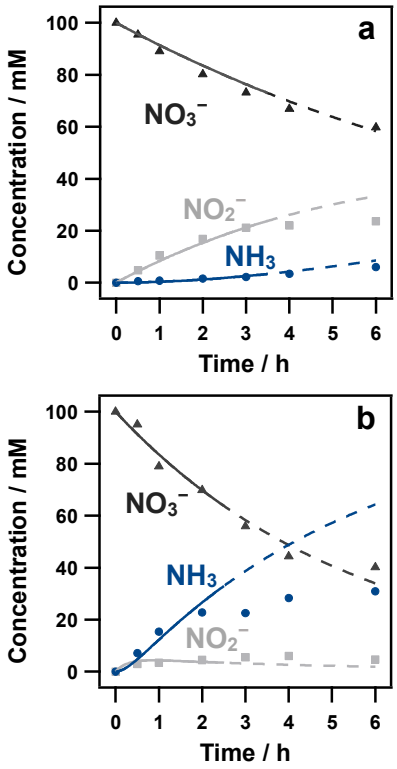

Figure 6. Time dependence of NO_3^- (black triangles), NO_2^- (gray squares) and NH_3 (blue dots), and corresponding fittings lines. Dashed fitting lines are for total (NO_3^-, NO_2^- and NH_3) concentration below 95 mM. Potentiostatic reduction at –1.8 V vs Ag/AgCl (KCl sat.) by using 0.2% BDD for 6 h: (a) 0.1 M $NaNO_3$, and (b) 0.1 M $NaNO_3$ added with 1 M NaOH. Divided batch cell, stirring rate 2912 rpm. WE: 12.56 cm^2.

The results obtained from the time-dependent concentrations are consistent with a coupled reaction that is a sequence of two elementary steps (eq 5):

$$NO_3^- \xrightarrow{k_1} NO_2^- \xrightarrow{k_2} NH_3 \quad (5)$$

Nitrate is firstly reduced to nitrite (k_1) that is subsequently reduced to ammonia (k_2). It is worth noting, that the reaction mechanism from nitrite to ammonia consists of several reaction steps as much as kinetic constants[13,21,27,32,64-67] included within k_2, indeed. Clearly dependent by the NaOH concentration, the rate of these two reactions can be modeled by a pseudo-first order equation (eqs 6–8):

$$\frac{d[NO_3^-]}{dt} = -k_1[NO_3^-] \quad (6)$$

$$\frac{d[NO_2^-]}{dt} = k_1[NO_3^-] - k_2[NO_2^-] \quad (7)$$

$$\frac{d[NH_3]}{dt} = k_2[NO_2^-] \quad (8)$$

which integrated give the time-dependent concentrations (eqs 9–11):

$$[NO_3^-] = [NO_3^-]_0 e_1^{-k_1 t} \quad (9)$$

$$[NO_2^-] = [NO_3^-]_0 \left\{ \frac{k_1}{k_2 - k_1} (e^{-k_1 t} - e^{-k_2 t}) \right\} \quad (10)$$

$$[NH_3] = [NO_3^-]_0 \left(1 - \frac{k_2}{k_2 - k_1} e^{-k_1 t} + \frac{k_1}{k_2 - k_1} e^{-k_2 t} \right) \quad (11)$$

The rate constants of this two steps reduction were $k_1 = 2.5 \times 10^{-5}$ s^{-1} and $k_2 = 2 \times 10^{-5}$ s^{-1}. The k_1 larger than k_2 suggests that electrochemical nitrate reduction reaction in $NaNO_3$ solution proceeds faster for production of nitrite than ammonia which explains the low faradaic efficiency for ammonia compared to nitrite without NaOH. However, when NaOH was added the two value of the constant rates swaps being $k_{1(NaOH)} = 5 \times 10^{-5}$ s^{-1} and $k_{2(NaOH)} = 1 \times 10^{-3}$ s^{-1} that are 2 times and 50 times higher than those without NaOH, respectively. This confirmed the faster reduction of nitrite to ammonia and the high selectivity for ammonia compared to nitrite by the addition of NaOH.

Clearly, the NH_3 concentration is lower than the theoretical value for time higher than 2 hours. Because the present system was tested under strong basic conditions (pH 13.48), slow N_2 bubbling and intense stirring, it is possible that NH_3 produced in the aqueous electrolyte could leak into the gas phase. This has been modeled by adding a third reaction of liquid NH_3 to gas NH_3 with $k_3 = 7 \times 10^{-5}$ s^{-1} (paragraph 17 in Supporting Information, and Figure S24). However, we cannot rule out completely the increasing formation of other undetected species, presumably hydrogen, which has been observed in batch electrolysis.[36]

Finally, the electrode kinetic of nitrate reduction was investigated by linear polarization to determine a possible mechanism, with the BDD electrode showing a Tafel slope of 72 mV dec^{-1} (Figure S25). Being near the theoretical value of 60 mV dec^{-1}, this implies a chemical rate-determining step.[68,69] Although it is difficult to rationalize a multistep electrochemical reaction mechanisms based on Tafel slope only,[70] similar low values for nitrate reduction reaction have been reported.[28,61]

BDD comparison and stability

To put the performance of BDD in perspective, other electrode materials were tested for NO_3^- reduction to NH_3 with our electrochemical setup (Table 1).

Table 1. Summary of ammonia production with different electrode materials. V *vs* Ag/AgCl (KCl sat.).

Electrode	P_{NH3} / μmol cm^{-2} h^{-1}	FE_{NH3} / %	E / V
Cu	243	57	–1.8
Ti	29	50	–1.26
Glassy carbon	86	92	–1.6
	156	57	–1.8

Copper is probably the most used metal for nitrate reduction, and in our conditions (i.e., 0.1 M $NaNO_3$ added with 1 M NaOH), it reached a P_{NH3} of 243.3 μmol cm^{-2} h^{-1} with a FE_{NH3} of 56.6% (Figure S26 and S27). Although the high current density enabled a substantial NH_3 production, this was associated with a deterioration of the NH_3 selectivity.

Titanium was tested according to a previous investigation in 0.3 M KNO_3 added with 0.1 M HNO_3 (pH 1.06) because this condition showed the best NH_3 production rate.[71] The P_{NH3} was 28.52 μmol cm^{-2} h^{-1} with a FE_{NH3} of 49.8% (Figure S26 and S27). For Ti, the comparison of the electrode before and after the nitrate reduction revealed a modification of the metal surface with the appearance of a brownish color (Figure S28), likely titanium hydride.[71]

Glassy carbon was tested to understand if carbon can be a suitable material, and also the difference between sp^3 and sp^2 hybridization in nitrate reduction. Surprisingly, glassy carbon could attain a FE_{NH3} of 92.0% with a P_{NH3} of 24 μmol cm^{-2} h^{-1} (Figure S29 and S30) which prompted our interest to assess its stability.

Continuous nitrate reduction of 6 hours for 5 times, and without surface cleaning at the conclusion of each 6 hours, revealed a degradation for the ammonia selectivity, with a FE_{NH3} from around 60% to 40%, with an almost stable P_{NH3} around 35 μmol cm^{-2} h^{-1}, although with a clear decreasing tendency (Figure S31 and S32). SEM imaging of the glassy carbon electrode revealed extended corrosion of the surface with increasing number of pores (Figure S33) that is responsible for the increasing current density (Figure S32). Furthermore, hindered diffusion of nitrate inside the pores can explain the decreasing FE_{NH3}, as the selectivity shifts toward hydrogen evolution.

In conclusion, the glassy carbon electrode is effective for electrochemical nitrate reduction, but its durability is insufficient.

The same stability test of glassy carbon applied to the BDD electrode did not reveal performance degradation, with a P_{NH3} around 35 μmol cm^{-2} h^{-1} (from 32 to 39 μmol cm^{-2} h^{-1}) and a FE_{NH3} around 50% (from 45.1% to 61.6%) with a slight tendency to increase (Figure S34 and S35). It is worth noting that the lower FE_{NH3} and P_{NH3} are only the result from long time experiment (6 h) compared to optimized experimental conditions (1 h).

By SEM imaging it was possible to exclude surface degradation by corrosion which is usually confirmed by gaps between the BDD crystals and rounded crystal edges (Figure S36).[72]

Moreover, Raman spectroscopy did not reveal significant chemical modifications (Figure S37). Generally, the degradation of BDD can be recognized from a shift of the sp^3 carbon peak around 1330 cm^{-1} to lower wavenumbers that has not been observed, as the sharp peak of sp^3 carbon set at 1329 cm^{-1}. A decrease in the intensity of the diamond disordered structure at 1200 cm^{-1} compared to the sp^3 carbon peak could occur,[72] alt-

hough only minor differences between the spectra were observed. While the sp^3 carbon structure was preserved, some impurities of amorphous sp^2 carbon at 1530 cm^{-1} were removed from the BDD surface, as revealed from the flattening of the large peak above 1500 cm^{-1}.[73]

Ammonia production rate enhancement

Attempts to increase the P_{NH3} were pursued by increasing the applied potential. From −1.8 V to −2.0 V the current increased, but the lower FE_{NH3} at 82% resulted in the same P_{NH3} which levelled at 67 μmol cm^{-2} h^{-1} (Figure 7, S38 and S39).

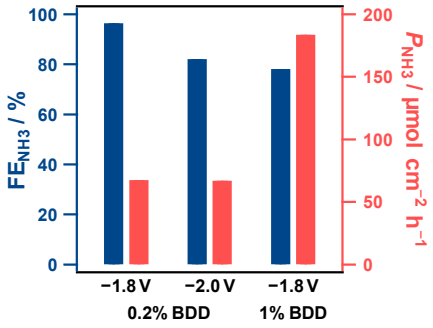

Figure 7. FE_{NH3} (blue) and P_{NH3} (red) from potentiostatic reduction of 0.1 M $NaNO_3$ added with 1 M NaOH using either 0.2% BDD (–1.8 V and –2.0 V), and 1% BDD (–1.8 V) for 1 h. Divided batch cell, stirring rate 2912 rpm. WE: 12.56 cm^2. V *vs* Ag/AgCl (KCl sat.).

The higher overpotential enhanced presumably the hydrogen evolution reaction instead of nitrate to ammonia.

Therefore, 1% BDD has been selected for further investigation of nitrate reduction owning its higher current compared to 0.2% BDD (Figure 1), because the higher boron concentration of BDD decreases the surface resistivity which facilitates the electron transfer with the species in solution.[53,54] Indeed, the P_{NH3} increased about 2.7 times, up to 184 μmol cm^{-2} h^{-1}, although the FE_{NH3} decreased to 78%. Again in this case, the hydrogen evolution reaction decreased the selectivity toward ammonia synthesis, but the production of harmful nitrite did not increase (Figure S38).

This suggests that the increase in current density of electrolysis due to the increase in electrode surface conductivity is more effective for ammonia production than the increase in overpotential (Figure S38).

Finally, a comparison of BDD with other materials revealed satisfactory results that combined with the stability of a bulk electrode like BDD contrary to metal (nano)electrocatalyst make the BDD a suitable material for electrochemical nitrate reduction to ammonia (Table S2).

CONCLUSION

We presented an investigation for the ammonia synthesis by electrochemical nitrate reduction by using a BDD electrode. Optimization of the boron doping concentration, reduction potential, and electrolyte showed that 0.2% BDD could reach a NH_3 production rate of 67±12 μmol cm^{-2} h^{-1} with a NH_3 faradaic efficiency of 98±6% at –1.8 V vs. Ag/AgCl in 0.1 M $NaNO_3$ added with 1 M NaOH under forced convection condition.

By a boron doping concentration of 1%, the NH_3 production rate could be enhanced by 2.7 times, up to 184 μmol cm^{-2} h^{-1}, although the FE_{NH3} decreased to 78%.

The addition of NaOH was effective to increase the electrolyte conductivity, and decrease the charge transfer resistance of the nitrate reduction, likely by facilitating the nitrate adsorption before the electron transfer.

This faster reduction reaction was confirmed by kinetic analysis from the time-dependent concentration of NO_3^-, NO_2^-, and NH_3. The NaOH enhanced the NO_3^- to NO_2^- reaction by 2 times, and NO_2^- to NH_3 reaction by 50 times.

A comparison with other electrodes (Cu, Ti, glassy carbon) confirmed that the BDD electrode is superior in terms of combined overall performances: production rate, faradaic efficiency, and durability.

As a final remark, the method proposed here for the synthesis of NH_3 should not be intended to substitute the Haber-Bosch process that possesses remarkable advantages, indeed. Rather it is a complementary process that can supply useful NH_3, and at the same time remove harmful nitrate/nitrite.

ASSOCIATED CONTENT

Supporting Information. Materials, BDD fabrication and characterization, electrochemical setup, electrochemical measurements, products analysis and spectroscopic measurements, data from literature for comparison. This material is available free of charge via the Internet at http://pubs.acs.org.

AUTHOR INFORMATION

Corresponding Author

*Andrea Fiorani - Department of Chemistry, Keio University, Yoko-hama 223-8522, Japan; orcid.org/0000-0001-8413-6439; Email: andrea.fiorani@keio.jp

*Yasuaki Einaga - Department of Chemistry, Keio University, Yoko-hama 223-8522, Japan; orcid.org/0000-0001-7057-4358; Email: einaga@chem.keio.ac.jp

Authors

Satoru Kuramochi - Department of Chemistry, Keio University, Yokohama 223-8522, Japan;

Author Contributions

The manuscript was written through contributions of all authors. All authors have given approval to the final version of the manuscript.

Funding Sources

This work was partially supported by Grant-in-Aid for Scientific Research A 23H00288 (to Y.E.).

Notes

The authors declare no competing financial interest.

ABBREVIATIONS

BDD, boron-doped diamond; MPCVD, microwave plasma-assisted chemical vapor deposition; LSV, linear sweep voltammetry; FE, faradaic efficiency; *P*, production rate.

REFERENCES

1 Tsipis, C. A.; Karipidis, P. A. Mechanistic Insights into the Bazarov Synthesis of Urea from NH_3 and CO_2 Using Electronic Structure Calculation Methods. *J. Phys. Chem. A* **2005**, *109* (38), 8560–8567.

2 Sorgenti, H. A.; Sachsel, G. F. Nitric Acid Manufacture—Theory and Practice. *Ind. Eng. Chem.* **1960**, *52* (2), 101–104.

3 Appl, M. Ammonia, 1. Introduction. In *Ullmann's Encyclopedia of Industrial Chemistry*, Wiley-VCH, **2011**. DOI: 10.1002/14356007.a02_143.pub3.

4 Chatterjee, S.; Parsapur, R. K.; Huang, K.-W. Limitations of Ammonia as a Hydrogen Energy Carrier for the Transportation Sector. *ACS Energy Lett.* **2021**, *6* (12), 4390–4394.

5 Leigh, G. J. Haber-Bosch and Other Industrial Processes. In *Catalysts for Nitrogen Fixation. Nitrogenases, Relevant Chemical Models and Commercial Processes*; Smith, B. E.; Richards, R. L.; Newton, W. E., Eds.; Nitrogen Fixation: Origins, Applications, and Research Progress, Vol. 1; Springer, **2004**; pp 33–54. DOI: 10.1007/978-1-4020-3611-8_2.

6 Humphreys, J.; Lan, R.; Tao, S. Development and Recent Progress on Ammonia Synthesis Catalysts for Haber–Bosch Process. *Adv. Energy Sustainability Res.* **2021**, *2* (1), 2000043.

7 Tang, X.; Hou, Y.; Nga, C. Y.; Ruscic, B. Pulsed field-ionization photoelectronphotoion coincidence study of the process $N_2+h\nu \rightarrow N^+ + N + e^-$: bond dissociation energies of N_2 and N_2^+. *J. Chem. Phys.* **2005**, *123* (7), 074330.

8 Kolen, M.; Ripepi, D.; Smith, W. A.; Burdyny, T.; Mulder, F. M. Overcoming Nitrogen Reduction to Ammonia Detection Challenges: The Case for Leapfrogging to Gas Diffusion Electrode Platforms. *ACS Catal.* **2022**, *12* (10), 5726–5735.

9 Chatt, J.; Leigh, G. J. Nitrogen fixation. *Chem. Soc. Rev.* **1972**, *1*, 121–144.

10 Li, K.; Shapel, S. G.; Hochfilzer, D.; Pedersen, J. B.; Krempl, K.; Andersen, S. Z.; Sažinas, R.; Saccoccio, M.; Li, S.; Chakraborty, D.; Kibsgaard, J.; Vesborg, P. C. K.; Nørskov, J. K.; Chorkendorff, I. Increasing Current Density of Li-Mediated Ammonia Synthesis with High Surface Area Copper Electrodes. *ACS Energy Lett.* **2022**, *7* (1), 36–41.

11 Sanginesi, F.; Millacci, G.; Giaccherini, A.; Buccianti, A.; Fusi, L.; Di Benedetto, F.; Pardi, L. Long term lithium availability and electric mobility: What can we learn from resource assessment?. *J. Geochem. Explor.* **2023**, *249*, 107212.

12 Tafel, J. Die elektrolytische Reduktion der Salpetersäure bei Gegenwart von Salzsäure oder Schwefelsäure. *Z. Anorg. Chem.* 1902, 31 (1), 289–325.

13 Martínez, J.; Ortiz, A.; Ortiz, I. State-of-the-art and perspectives of the catalytic and electrocatalytic reduction of aqueous nitrates. *Appl. Catal., B* **2017**, *207*, 42–59.

14 van Langevelde, P. H.; Katsounaros, I.; Koper, M. T. M. Electrocatalytic Nitrate Reduction for Sustainable Ammonia Production, Joule **2021**, *5* (2), 290–294.

15 Camargo, J. A.; Alonso, A. Ecological and toxicological effects of inorganic nitrogen pollution in aquatic ecosystems: A global assessment. Environ. Int. **2006**, *32* (6), 831–849.

16 Kuypers, M. M. M.; Marchant, H. K.; Kartal, B. The microbial nitrogen-cycling network. *Nat. Rev. Microbiol.* **2018**, *16* (5), 263–276.

17 Genders, J. D.; Hartsough, D.; Hobbs, D. T. Electrochemical reduction of nitrates and nitrites in alkaline nuclear waste solutions. *J. Appl. Electrochem.* **1996**, *26* (1), 1–9.

18 Katsounaros, I.; Dortsiou, M.; Kyriacou, G. Electrochemical reduction of nitrate and nitrite in simulated liquid nuclear wastes. *J. Hazard. Mater.* **2009**, *171* (1–3), 323–327.

19 Ferro, S. Removal of Nitrates from Industrial Wastewater. *Chim. Ind.* **2012**, *2*, 100–110.

20 Carliell, C. M.; Barclay, S. J.; Shaw, C.; Wheatley, A. D.; Buckley, C. A. The Effect of Salts Used in Textile Dyeing on Microbial Decolourisation of a Reactive Azo Dye. *Environ. Technol.* **1998**, *19* (11), 1133–1137.

21 Rosca, V.; Duca, M.; de Groot, M. T.; Koper, M. T. M. Nitrogen Cycle Electrocatalysis. *Chem. Rev.* **2009**, *109* (6), 2209–2244.

22 Pourbaix, M. *Atlas of Electrochemical Equilibria in Aqueous Solutions*, 2nd ed.; National Association of Corrosion: Houston, 1974.

23 Bratsch, S. G. Standard Electrode Potentials and Temperature Coefficients in Water at 298.15 K. *J. Phys. Chem. Ref. Data* **1989**, *18* (1), 1–21.

24 Barrera, L.; Silcox, R.; Giammalvo, K.; Brower, E., Isip, E.; Chandran, R. B. Combined Effects of Concentration, pH, and Polycrystalline Copper Surfaces on Electrocatalytic Nitrate-to-Ammonia Activity and Selectivity. *ACS Catal.* **2023**, *13* (7), 4178–4192.

25 Ren, Z.; Shi, K.; Feng, X. Elucidating the Intrinsic Activity and Selectivity of Cu for Nitrate Electroreduction. *ACS Energy Lett.* **2023**, *8* (9), 3658–3665.

26 Wang, Y.; Zhou, W.; Jia, R.; Yu, Y.; Zhang, B. Unveiling the Activity Origin of a Copper-based Electrocatalyst for Selective Nitrate Reduction to Ammonia. *Angew. Chem. Int. Ed.* **2020**, *59* (13), 5350–5354.

27 Zhang, J.; He, W.; Quast, T.; Junqueira, J. R. C.; Saddeler, S.; Schulz, S.; Schuhmann, W. Single-entity Electrochemistry Unveils Dynamic Transformation during Tandem Catalysis of Cu2O and Co3O4 for Converting NO3− to NH3. *Angew. Chem. Int. Ed.* **2023**, *62* (8), e202214830.

28 He, W.; Zhang, J.; Dieckhöfer, S.; Varhade, S.; Brix, A. C.; Lielpetere, A.; Seisel, S.; Junqueira, J. R. C.; Schuhmann, W. Splicing the active phases of copper/cobalt-based catalysts achieves high-rate tandem electroreduction of nitrate to ammonia. *Nat. Commun.* **2022**, *13*, 1129.

29 Du, Z.; Yang, K.; Du, H.; Li, B.; Wang, K.; He, S.; T., Ai, W. W. Facile and Scalable Synthesis of Self-Supported Zn-Doped CuO Nanosheet Arrays for Efficient Nitrate Reduction to Ammonium. *ACS Appl. Mater. Interfaces* **2023**, *15* (4), 5172-5179.

30 Mattarozzi, L.; Cattarin, S.; Comisso, N.; Gambirasi, A.; Guerriero, P.; Musiani, M.; Vázquez-Gómez, L.; Verlato, E. Hydrogen evolution assisted electrodeposition of porous Cu-Ni alloy electrodes and their use for nitrate reduction in alkali. *Electrochim. Acta* **2014**, *140*, 337–344.

31 Comisso, N.; Cattarin, S.; Fiameni, S.; Gerbasi, R.; Mattarozzi, L.; Musiani, M.; Vázquez-Gómeza, L.; Verlato, E.; Electrodeposition of Cu–Rh alloys and their use as cathodes for nitrate reduction. *Electrochem. Commun.* **2012**, *25* (1), 91–93.

32 Crawford, J.; Yin, H.; Du, A.; O'Mullane, A. P. Nitrate-to-Ammonia Conversion at an InSn-Enriched Liquid-Metal Electrode. *Angew. Chem. Int. Ed.* **2022**, *61* (23), e202201604.

33 Wu, Z.-Y.; Karamad, M.; Yong, X.; Huang, Q.; Cullen, D. A.; Zhu, P.; Xia, C.; Xiao, Q.; Shakouri, M.; Chen, F.-Y.; Kim, J. Y.; Xia, Y.; Heck, K.; Hu, Y.; Wong, M. S.; Li, Q.; Gates, I.; Siahrostami, S.; Wang, H. Electrochemical ammonia synthesis via nitrate reduction on Fe single atom catalyst. *Nat. Commun.* **2021**, *12*, 2870.

34 Zhang, G.; Li, X.; Chen, K.; Guo, Y.; Ma, D.; Chu, K. Tandem Electrocatalytic Nitrate Reduction to Ammonia on MBenes. *Angew. Chem. Int. Ed.* **2023**, *62* (13), e202300054.

35 Guo, Y.; Cai, X.; Shen, S.; Wang, G.; Zhang, J. Computational prediction and experimental evaluation of nitrate reduction to ammonia on rhodium. *J Catal.* **2021**, *402*, 1-9.

36 Mattarozzi, L.; Cattarin, S.; Comisso, N.; Musiani, M.; Vázquez-Gómez, L.; Verlato, E. Electrodeposition of Ni−Rh Alloys and their Use as Cathodes for Nitrate Reduction in Alkaline Solutions. *ChemElectroChem* **2023**, *10* (6), e202201122.

37 Liu, H.; Park, J.; Chen, Y.; Qiu, Y.; Cheng, Y.; Srivastava, K.; Gu, S.; Shanks, B. H.; Roling, L. T., Li, W. Electrocatalytic Nitrate Reduction on Oxide-Derived Silver with Tunable Selectivity to Nitrite and Ammonia. *ACS Catal.* **2021**, *11* (14), 8431−8442.

38 Xu S.; Shi, Y.; Wen, Z.; Liu, X.; Zhu, Y.; Liu, G.; Gao, H.; Sun, L.; Li, F. Polystyrene spheres-templated mesoporous carbonous frameworks implanted with cobalt nanoparticles for highly efficient electrochemical nitrate reduction to ammonia. *Appl. Catal., B* **2023**, *323*, 122192.

39 Guo, Y.; Zhang, R.; Zhang, S., Zhao, Y.; Yang, Q.; Huang, Z.; Dong, B.; Zhi, C. Pd doping-weakened intermediate adsorption to promote electrocatalytic nitrate reduction on TiO2 nanoarrays for ammonia production and energy supply with zinc–nitrate batteries. *Energy Environ. Sci.* **2021**, *14* (7), 3938–3944.

40 Fan, X.; Ma, C.; Zhao, D.; Deng, Z.; Zhang, L.; Wang, Y.; Luo, Y.; Zheng, D.; Li, T.; Zhang, J.; Sun, S.; Lu, Q., Sun, X. Unveiling selective nitrate reduction to ammonia with Co3O4 nanosheets/TiO2 nanobelt heterostructure catalyst. *J. Colloid Interface Sci.* **2023**, *630* (Part A), 714–720.

41 Li, F.-M.; Huang, L.; Zaman, S.; Guo, W.; Liu, H.; Guo, X.; Xia, B. Y. Corrosion Chemistry of Electrocatalysts *Adv. Mater.* **2022**, *34*, 2200840.

42 Yang, N.; Yu, S., Macpherson, J. V.; Einaga, Y.; Zhao, H.; Zhao, G.; Swain, G. M.; Jiang, X. Conductive diamond: synthesis, properties, and electrochemical applications. *Chem. Soc. Rev.* **2019**, *48* (1), 157–204.

43 Swain, G. M.; Ramesham, R. The electrochemical activity of boron-doped polycrystalline diamond thin film electrodes. *Anal. Chem.* **1993**, *65* (4), 345–351.

44 Einaga, Y. Diamond electrodes for electrochemical analysis. *J. Appl. Electrochem.* **2010**, *40* (10), 1807–1816.

45 Einaga, Y. Boron-Doped Diamond Electrodes: Fundamentals for Electrochemical Applications. *Acc. Chem. Res.* **2022**, *55* (24), 3605–3615.

46 Einaga, Y. Application of Boron-doped Diamond Electrodes: Focusing on the Electrochemical Reduction of Carbon Dioxide. *Electrochemistry* **2022**, *90* (10), 101002.

47 Iwai, G.; Fiorani, A.; Du, J.; Einaga, Y. Photo-assisted electrochemical CO_2 reduction at a boron-doped diamond cathode. *Energy Adv.* **2023**, *2* (5), 733–738.

48 Du, J.; Fiorani, A.; Inagaki, T.; Otake, A.; Murata, M.; Hatanaka, M.; Einaga, Y. A New Pathway for CO_2 Reduction Relying on the Self-Activation Mechanism of Boron-Doped Diamond Cathode. *JACS Au* **2022**, *2* (6), 1375–1382.

49 Peng, Z.; Fiorani, A.; Tomisaki, M.; Nishide, Y.; Hagiwara, M.; Fujihara, S.; Einaga, Y. Morphology modulation on boron-doped diamond electrodes and its effect on boosting the conversion of CO_2-to-CO. *Diamond Relat. Mater.* **2023**, *138*, 110230.

50 Du, J.; Fiorani, A.; Einaga, Y. Electrochemical CO_2 reduction to CO facilitated by reduced boron-doped diamond. *Diamond Relat. Mater.* **2023**, *135*, 109902.

51 Nielsen, F. H. Boron in human and animal nutrition. Plant and Soil **1997**, *193* (1–2), 199–208.

52 Calzaferri, G.; Rytz, R. The Band Structure of Diamond. *J. Phys. Chem.* **1996**, *100* (26), 11122–11124

53 Lagrange, J.-P.; Deneuville, A.; Gheeraert, E. Activation energy in low compensated homoepitaxial boron-doped diamond films. *Diamond Relat. Mater.* **1998**, *7* (9), 1390–1393.

54 Sakanoue, K.; Fiorani, A.; Irkham; Einaga, Y. Effect of Boron-Doping Level and Surface Termination in Diamond on Electrogenerated Chemiluminescence. *ACS Appl. Electron. Mater.* **2021**, *3* (9), 4180–4188.

55 Kuang, P.; Natsui, K.; Feng, C.; Einaga, Y. Electrochemical reduction of nitrate on boron-doped diamond electrodes: Effects of surface termination and boron-doping level. *Chemosphere* **2020**, *251*, 126364.

56 Ramaswamy, N.; Mukerjee, S. Influence of Inner- and Outer-Sphere Electron Transfer Mechanisms during Electrocatalysis of Oxygen Reduction in Alkaline Media. *J. Phys. Chem. C* **2011**, **115** (36), 18015–18026.

57 Ge, X.; Sumboja, A.; Wuu, D., An, T.; Li, B.; Goh, F. W. T.; Hor, T. S. A.; Zong, Y.; Liu, Z. Oxygen Reduction in Alkaline Media: From Mechanisms to Recent Advances of Catalysts. *ACS Catal.* **2015**, *5* (8), 4643–4667.

58 Petrii, O. A.; Safonova, T. Ya. Electroreduction of nitrate and nitrite anions on platinum metals: a model process for elucidating the nature of the passivation by hydrogen adsorption. *J. Electroanal. Chem.* **1992**, 331 (1–2), 897–912.

59 Safonova, T. Ya.; Petrii, O. A. Effect of inorganic cations on the electroreduction of nitrate anions on Pt|Pt electrodes in sulfuric acid solutions. *J. Electroanal. Chem.* **1998**, *448* (2), 211–216.

60 Ohmori, T.; El-Deab, M. S.; Osawa, M. Electroreduction of nitrate ion to nitrite and ammonia on a gold electrode in acidic and basic sodium and cesium nitrate solutions. *J. Electroanal. Chem.* **1999**, *470* (1), 46–52.

61 Dima, G. E.; de Vooys, A. C. A.; Koper, M. T. M. Electrocatalytic reduction of nitrate at low concentration on coinage and transition−metal electrodes in acid solutions. *J. Electroanal. Chem.* **2003**, *554–555*, 15–23.

62 Kasahara, S.; Natsui, K.; Watanabe, T.; Yokota, Y.; Kim; Y.; Iizuka, S.; Tateyama, Y.; Einaga, Y. Surface Hydrogenation of Boron-Doped Diamond Electrodes by Cathodic Reduction. *Anal. Chem.* **2017**, *89* (21), 11341–11347.

63 Kuang, P.; Natsui, K.; Feng, C.; Einaga, Y. Electrochemical reduction of nitrate on boron-doped diamond electrodes: Effects of surface termination and boron-doping level. *Chemosphere* **2020**, *251*, 126364.

64 Kuwabata, S.; Uezumi, S.; Tanaka, K.; Tanaka, T. Assimilatory and Dissimilatory Reduction of NO3– and NO2– with an (*n*-Bu4N)3[Mo2Fe6S8(SPh)9] Modified Glassy-Carbon Electrode in Water. *Inorg. Chem.* **1986**, *25* (17), 3018-3022.

65 Tanaka, K.; Komeda, N.; Matsui, T. Electrochemical assimilatory and dissimilatory reductions of nitrate and nitrite via a possible free nitric oxide intermediate. *Inorg. Chem.* **1991**, *30* (17), 3282–3288.

66 Wasmus, S.; Vasini, E. J.; Krausa, M.; Mishima, H. T.; Vielstich, W. DEMS-cyclic voltammetry investigation of the electrochemistry of nitrogen compounds in 0.5 M potassium hydroxide. *Electrochim. Acta* **1994**, *39* (1), 23–31.

67 Gootzen, J. F. E.; Peeters, P. G. J. M.; Dukers, J. M. B.; Lefferts, L.; Visscher, W.; van Veen, J. A. R. The electrocatalytic reduction of NO3– on Pt, Pd and Pt + Pd electrodes activated with Ge. *J. Electroanal. Chem.* **1997**, *434* (1–2), 171–183

68 Fang, Y.-H.; Liu, Z.-P. Tafel Kinetics of Electrocatalytic Reactions: From Experiment to First Principles. *ACS Catal.* **2014**, *4* (12), 4364−4376.

69 Petrii, O. A.; Nazmutdinov, R. R.; Bronshtein, M. D.; Tsirlina, G. A. Life of the Tafel equation: Current understanding and prospects for the second century. *Electrochim. Acta* **2007**, *52* (11), 3493−3504.

70 Lefebvre, M. C. Establishing the Link Between Multistep Electrochemical Reaction Mechanisms and Experimental Tafel Slopes. In *Modern Aspects of Electrochemistry*; Conway, B. E., Bockris, J. O., White, R. E., Eds.; Modern Aspects of Electrochemistry book series, Vol. 32; Springer, Boston, MA, 2002; pp 249−300. DOI: 10.1007/0-306-46916-2_3.

71 McEnaney, J. M.; Blair, S. J.; Nielander, A. C.; Schwalbe, J. A.; Koshy, D. M.; Cargnello, M.; Jaramillo, T. F. Electrolyte Engineering for Efficient Electrochemical Nitrate Reduction to Ammonia on a Titanium Electrode. *ACS Sustainable Chem. Eng.* **2020**, *8* (7), 2672–2681.

72 Kashiwada, T.; Watanabe, T., Ootani, Y.; Tateyama, Y.; Einaga, Y. A Study on Electrolytic Corrosion of Boron-Doped Diamond Electrodes when Decomposing Organic Compounds. *ACS Appl. Mater. Interfaces* **2016**, *8* (42), 28299–28305.

73 Xu, J.; Yokota, Y.; Wong, R. A.; Kim, Y.; Einaga, Y. Unusual Electrochemical Properties of Low-Doped Boron-Doped Diamond Electrodes Containing sp2 Carbon. *J. Am. Chem. Soc.* **2020**, *142* (5), 2310–2316.

SYNOPSIS TOC

Electrochemical Synthesis of Ammonia by Boron-Doped Diamond